Co-ordination Chemistry of Adenine (HAde): Synthesis and Characterization of $[Cu^{II}(tren)(nucleobase)]X_2$ [tren = tris-(2-aminoethyl)amine, X = Cl or NO_3] Complexes and Crystal Structure of $[Cu^{II}(tren)(Ade)]Cl\cdot 2H_2O$ †

Armando Marzotto,[a] Antonella Ciccarese,[b] Dore A. Clemente[c] and Giovanni Valle[d]

[a] *Dipartimento di Chimica Inorganica, Metallorganica ed Analitica, Università di Padova, Via Loredan 4, 35131 Padova, Italy*

[b] *Dipartimento di Biologia, Facoltà di Scienze, Univeristà di Lecce, Via Monteroni, 73100 Lecce, Italy*

[c] *Dipartimento di Ingegneria dei Materiali e di Chimica Applicata, Università di Trieste, Via Valerio 2, 34127 Trieste, Italy*

[d] *Centro di Studio sui Biopolimeri, C.N.R., Università di Padova, Via Marzolo 1, 35131 Padova, Italy*

The five-co-ordinate complexes $[Cu^{II}(tren)(H_2O)]Cl_2$ **1**, $[Cu^{II}(tren)(HAde)]Cl_2$ **2**, $[Cu^{II}(tren)(HAde)][NO_3]_2$ **3** and $[Cu^{II}(tren)(Ade)]Cl\cdot 2H_2O$ **4** [tren = tris(2-aminoethyl)amine and HAde = neutral adenine] have been synthesized and characterized. The geometry and structures of the complexes were studied by electronic and IR spectra and, in addition, the structure of complex **4** has been determined by X-ray crystallography. The physicochemical data for complexes **2** and **3** support the presence of neutral adenine co-ordinated to Cu^{II}, whereas in complex **4** the adenine molecule is bound in its monoanionic form, as confirmed by the X-ray analysis [monoclinic, space group $P2_1/a$, $a = 15.001(2)$, $b = 8.422(1)$, $c = 15.039(2)$ Å, $\beta = 105.90(6)°$, $Z = 4$; $R = 0.065$ for 2596 unique diffraction data]. The co-ordination polyhedron around the Cu^{2+} ion is approximately trigonal bipyramidal, with the equatorial sites occupied by the three primary amino nitrogen atoms and the axial positions occupied by the tertiary amino nitrogen and the imidazole N^9 nitrogen from the adenine monoanion. The Cu–N(9) distance is rather short at 1.965(9) Å. Such selective metal bonding in adenine is very probably promoted by the trigonal-bipyramidal geometry around Cu^{II} and by the relatively low steric hindrance of the Cu^{II}(tren) moiety.

The co-ordination chemistry of adenine (in its various forms: adenine monoanion, neutral adenine, adenine monocation and adenine dication) is of great interest since this purine base, contained in DNA in relative amounts depending on genetic, evolutive and polluting factors, possesses nitrogen sites suitable for hydrogen and metal binding. Moreover, the target for anti-cancer pharmaceuticals containing platinum and some other metals probably involves adenine.

It is known that adenine (in its various forms) can co-ordinate to metal ions through all five of its nitrogen atoms, *i.e.* N^1, N^3, N^6, N^7 and N^9, but binding occurs preferentially at the imidazole N^9 atom. When N^9 is bound to an alkyl or ribosyl group and thus is no longer available for metal co-ordination, N^7 becomes the preferential binding site and only subsequently are the other nitrogen-binding sites involved.[1,2]

There is growing interest in the interaction of metal ions with nucleotides and nucleic acids. In the last few years there have been advances[3,4] in addressing metal ions to bind selectively to particular nitrogen sites of DNA nucleobases by using metal complexes with different steric hindrances and hydrogen bonding capabilities. Since our interest is in DNA metal–nucleotide binding, we have prepared and characterized, also by X-ray diffraction, some metal complexes of the tetradentate ligand tris(2-aminoethyl)amine (tren) with various steric hindrances and hydrogen bonding, such as Ni^{II} complexes with octahedral geometry or Cu^{I}, Cu^{II} and Zn^{II} with trigonal-bipyramidal geometry. We have demonstrated by X-ray crystallography that the bulky octahedral complex $[Ni(tren)(H_2O)Cl]Cl\cdot H_2O$[5] can react with adenine (HAde) and selectively recognize its pyrimidine N^3 nitrogen, forming octahedral [Ni(tren)(HAde)Cl]Cl in which a new exclusive Ni–N^3 pyrimidine bond does occur.[4] In order to check the molecular recognition of DNA nitrogen-binding sites by tren metal complexes and in particular to verify whether the N^3 nitrogen is also the preferential binding site for five-co-ordinate complexes with lower steric hindrance, we have synthesized and studied the following complexes: $[Cu^{II}(tren)(H_2O)]Cl_2$ **1**, $[Cu^{II}(tren)(HAde)]Cl_2$ **2**, $[Cu^{II}(tren)(HAde)][NO_3]_2$ **3** and $[Cu^{II}(tren)(Ade)]Cl\cdot 2H_2O$ **4**. In addition the crystal and molecular structure of complex **4** has been determined.

The chemical investigation of the binding of neutral adenine to metal tren complexes is also of interest from a biological point of view, since free adenine is present in various human and animal tissues, where the appropriate intracellular phospho-

Table 1 Approximate absorption maxima (cm^{-1}) in the electronic spectra of trigonal-bipyramidal Cu^{II} complexes

Complex	$10^{-3}\ \tilde{\nu}/cm^{-1}$	
$[Cu(tren)(NH_3)][ClO_4]_2$ [a]	11.4	15.2 (sh)
[Cu(hmtren)Br]Br [b]	10.4	13.3
$[Cu(hmtren)(ClO_4)]ClO_4$ [c]	11.2	13.8 (sh)
$[Cu(hmtren)(NO_3)]NO_3$ [c]	11.2	14.3 (sh)
$[Cu(tren)(H_2O)]Cl_2$ [d]	11.4	13.8 (sh)
$[Cu(tren)(HAde)]Cl_2$ [d]	12.4	15.4 (sh)
$[Cu(tren)(HAde)][NO_3]_2$ [d]	12.5	15.4 (sh)
$[Cu(tren)(Ade)]Cl\cdot 2H_2O$ [d]	12.5	15.4 (sh)

[a] Polycrystalline, ref. 7. [b] In $CHCl_3$. [c] In $EtNO_2$, ref. 6. [d] In EtOH, this work.

† *Supplementary data available:* see Instructions for Authors, *J. Chem. Soc., Dalton Trans.*, 1995, Issue 1, pp. xxv–xxx.

Table 2 Infrared spectra (cm^{-1}) of adenine, tren, $[Cu(tren)(H_2O)]Cl_2$ and metal complexes containing neutral adenine and monoanionic adenine

HAde[a–c]	$[Cu(HAde)_2(ClO_4)_2]\cdot EtOH$[a]	tren[d]	$[Cu(tren)(H_2O)]Cl_2$ **1**	[Ni(tren)(HAde)-Cl]Cl[e]	[Cu(tren)(HAde)]-Cl_2 **2**	[Cu(tren)(HAde)]-$[NO_3]_2$ **3**	Band assignment
3350 (sh), 3294s, 3118s	3620–3300ms (vbr)	3350s, 3270s, 3180m	3425s (br), 3373 (sh), 3265s(sh), 3221vs, 3194 (sh), 3122m (br)	3320s (br), 3298 (sh), 3250s, 3086m, 3030w (br)	3396m (br), 3337m, 3291s, 3248ms, 3144m, 3123s, 3050 (sh)	3427m (sh), 3310s, 3252s, 3124s (br)	$\nu(O–H) + \nu(NH_2)_{tren} + \nu(NH_2)_{arom}$
2985s, 2900m, 2800m, 2690m, 2600m	2700w, 2590w	2930s, 2855s, 2800s	2970 (sh), 2948m, 2924 (sh), 2886m	2983w, 2910w, 2874w, 2858w, 2827w, 2690w, 2660w	2975m, 2951m, 2918w, 2853w, 2746w, 2705w, 2675w, 2620w, 2592w, 2564w	2984ms, 2949 (sh), 2917w, 2891mw, 2872w, 2827 (sh), 2795m, 2750w, 2709w, 2688m, 2598w, 2569vw	$\nu(C–H)_{arom} + \nu(CH_2)_{tren} + \nu(N–H)_{arom}$
1673vs	1659vs		1635mw	1675vs, 1658vs	1669m, 1661ms	1669s	$\delta(NH_2)_{arom}$[f] + δ(HOH)
1604vs, 1570s, 1507w, 1449m, 1420s, 1367m, 1331s, 1309vs	1632s (sh), 1614s (sh), 1581s, 1509ms (br), 1460m, 1445s, 1409s, 1387w, 1363s, 1340m, 1319s	1590s (br), 1445m, 1390w, 1365 (sh), 1348m, 1304m	1593vs, 1578s (sh), 1477s, 1457m, 1441 (sh), 1398w, 1381mw, 1355w, 1322ms, 1303 (sh)	1609vs, 1564vs, 1515m, 1482s, 1475 (sh), 1450s, 1396s, 1359m, 1336s, 1315m	1598s, 1544w, 1525w, 1510w, 1464m, 1450 (sh), 1418m, 1387m, 1368w, 1336m, 1311m	1603s, 1545m, 1508w, 1471 (sh), 1463m, 1418ms, 1385s, 1365s, 1333s, 1308s	$\delta(NH_2)_{tren} + \nu(C{=}C) + \nu(C{=}N) + \delta(CH_2) + \gamma(CH_2)$ + ring vibrations
1250s, 1235 (sh), 1156w, 1125m	1258m, 1219ms, 1141vs	1270m, 1230w, 1112vs	1287vw, 1259mw, 1242w, 1182ms, 1108s	1293 (sh), 1248s, 1221 (sh), 1165m, 1125w	1294 (sh), 1254w, 1238w, 1199ms, 1137w, 1115w	1292 (sh), 1252m, 1236 (sh), 1203ms, 1144w, 1125w	$\nu(C–NH_2) + \nu(C–N)$ or $\delta(N^9–H)$ + ring mode
1023m	1085vs, 1036m	1090m, 1070w, 1035s, 1020 (sh)	1080s, 1057s, 1036s, 1015vs	1100 (sh), 1082 (sh), 1055s, 1038m, 1010 (sh), 1004s	1091vw, 1058m, 1041m, 1017w	1098w, 1061m, 1042w, 1020m	$\rho(NH_2)$ region
	970w		998vs, 950m, 898m	979s, 947m	992m, 974m	995m, 976m	
939s, 912s	930m, 922m (sh), 902m	902s (br), 865s (br), 840 (sh)		920w, 910w, 895m	940m, 902mw	939m, 911m	NH_2 deformation[f] + ring mode
871m, 847m, 796w	885w (br)		878w	883m, 859w, 847w	870w, 847w	870w, 846w	NH_2 rock + ring skeleton vibrations
723s	790ms, 731w, 680w (br)	765 (sh), 730w	768m, 713w, 667w	792ms, 743m, 734m, 692w, 661m	801mw, 740 (sh), 733vw, 722mw, 696vw, 687vw, 674vw, 641m	797m, 746w, 723m, 700vw, 651m, 642w	NH_2 deformation[f]
645w, 639s, 621w, 542m, 530vw, 337m, 248w, 225m (br)	639s, 628s, 621m (sh)		599mw, 533ms, 502s, 266m, 253m	625w, 611s, 578w, 562m, 538m, 532m, 508w, 470m, 345m, 335s (br)	622w, 565w, 546m, 342m, 337w, 303w, 267mw, 294w, 221 (sh)	623w, 572mw, 567mw, 542ms, 507w, 345w, 336ms, 303w, 263w, 247m, 221w	Main skeleton vibrations (adenine ring and tren chain)
			464m[g]				$\nu(Cu–OH_2)$
			467w, 464m,[g] 452m, 442w	362m, 314m, 301m, 285w (br)	472 (sh), 464ms, 450ms, 442w	486w, 474mw, 458w, 453w, 436 (sh)	$\nu(M–N_{tren})$[h]
	290s, 280s, 259m			258 (sh) 252m	284w, 257mw, 233m	278vw, 254w, 227w	$\nu(M–N_{arom})$[h] ν(Ni–Cl)

Table 2 (*contd.*)

[Ni(Ade)(ClO_4)]·EtOH·2H_2O[a]	[Ni_2(Ade)$_3$Cl]·6H_2O[c]	[Cu(Ade)(HAde)Cl]·H_2O[c]	[Cu(tren)(Ade)]Cl·2H_2O **4**	Band assignment
3390ms (vbr)	3390m (sh), 3310vs (br), 3105vs	3470m, 3360vs (sh), 3310vs, 3115vs	3400ms (br), 3332m, 3291m, 3244ms, 3144m	ν(O–H) + $\nu(NH_2)_{tren}$ + $\nu(NH_2)_{arom}$
	3000s (sh) 2640w (br)	2990vs, 2930s (sh), 2790s, 2680s, 2590s	2975m, 2923w, 2891m, 2850 (sh), 2712w	$\nu(C–H)_{arom}$ + $\nu(CH_2)_{tren}$ + $\nu(N–H)_{arom}$
1637s	1662vs	1672vvs	1664s	$\delta(NH_2)_{arom}$[f] + δ(HOH)
1622m (sh), 1604s, 1570s, 1525s (br), 1468m, 1440s, 1399s, 1380m (vbr), 1347s, 1329s	1648s, 1606vs, 1570s (br), 1540m (sh), 1440m, 1397m (br), 1350m, 1300s	1650vs, 1608vs, 1562s (sh), 1538m, 1450m, 1416m, 1403m, 1360mw, 1331m, 1304ms	1602s, 1544w, 1486 (sh), 1464m, 1450 (sh), 1418w, 1388m, 1363w, 1336w, 1316m, 1300 (sh)	$\delta(NH_2)_{tren}$ + ν(C=C) + ν(C=N) + $\delta(CH_2)$ + $\gamma(CH_2)$ + ring vibrations
1225m (br)	1254m	1250m	1262mw, 1240 (sh), 1201ms, 1104w	ν(C–NH_2) + ν(C–N) + NH_2 deformation[f] + ring mode
	1085w, 1022m	1090w, 1018m	1059m, 1044 (sh), 1016w	$\rho(NH_2)$ region
957w			995w, 975w	
902m			940w, 903m	NH_2 deformation[f] + ring mode
860w (sh)			870w, 819 (sh), 801w	NH_2 rock + ring skeleton vibrations
787w (br), 700w (br)			748w, 726vw, 704vw	NH_2 deformation[f]
	530m, 445m (br), 340w, 322w, 266w (sh)	535m, 440m (sh), 327m, 225w (br)	652w, 642w, 573w, 563w, 544ms, 344m	Main skeleton vibrations (adenine ring and tren chain)
	407m (br)	460m		ν(M–OH_2)[h]
			496m, 484m, 471m, 466m, 460w, 442w	ν(Cu–N_{tren})
	255m, 244m	303m, 286mw		ν(M–Cl)[h]
262ms, 227vs	240w, 221w	280ms, 261mw	300mw, 260mw	ν(M–N_{arom})[h]

[a] Ref. 10. [b] Ref. 11. [c] Ref. 12. [d] Ref. 13. [e] Ref. 4. [f] NH_2 deformation modes in HAde: sym. in-plane 1673; asym. out-of-plane 1250; sym. out-of-plane 939; asym. in-plane 723 cm^{-1}, ref. 10. [g] Overlapping bands. [h] M = Ni or Cu.

ribosyl-transferase enzyme contributes to the salvage of adenine by catalysing its phosphoribosylation at the N^9 site to form adenosine 5′-monophosphate (AMP).[6] Furthermore, free adenine or its N^6-substituted derivatives are also present in vegetable cells, for instance the cytokinins, a class of N^6-substituted adenine derivatives, are contained in plants and play an important role as phytohormones.[7]

Results and Discussion

Electronic Spectra.—The assignment of electronic absorption spectra for trigonal-bipyramidal copper(II) complexes has been discussed extensively in the literature.[8,9] The absorption maxima observed in the visible electronic spectra of $[Cu^{II}(tren)(H_2O)]Cl_2$ **1**, $[Cu^{II}(tren)(HAde)]Cl_2$ **2**, $[Cu^{II}(tren)(HAde)][NO_3]_2$ **3** and $[Cu^{II}(tren)(Ade)]Cl{\cdot}2H_2O$ **4** are compared in Table 1 with those of trigonal-bipyramidal $[Cu(tren)(NH_3)][ClO_4]_2$ and [Cu(hmtren)X]X (hmtren = hexamethylamino derivative of tren; X = Br^-, ClO_4^- or NO_3^-).[8,9] The visible spectra of complexes **1**–**4** show the same features found for five-co-ordinate complexes of a d^9 ion in a trigonal-bipyramidal field, *i.e.* two characteristic broad peaks occur at frequencies very close to those reported for trigonal-bipyramidal Cu^{II} complexes. In agreement with Duggan *et al.*,[9] it is therefore reasonable to assign the intense bands at 11 400 (**1**), 12 400 (**2**), 12 500 (**3**) or 12 500 (**4**) cm^{-1} respectively to the $d_{xy},d_{x^2-y^2} \longrightarrow d_{z^2}$ transition which is allowed in C_3 and D_{3h}, and the less intense shoulders at 13 800 (**1**), 15 400 (**2**), 15 400 (**3**) or 15 400 (**4**) cm^{-1} respectively to the $d_{xy},d_{yz} \longrightarrow d_{z^2}$ transition which, although allowed in C_3 symmetry, is forbidden in D_{3h} but which may occur weakly by a vibronic mechanism. This assignment is in agreement with that suggested for analogous solid trigonal-bipyramidal copper(II) complexes,[9] so that the close similarity of the spectra for the present complexes in ethanol with those of the solid-state complexes also indicates that their stereochemistry does not change appreciably on dissolution.

The formulation of complex **1** as $[Cu^{II}(tren)(H_2O)]Cl_2$ is strongly supported by thermogravimetric measurements (see Experimental section) which indicate that the H_2O molecule occupies the fifth co-ordination position to Cu^{II}.

The neutral adenine molecule is able to substitute the co-ordinated water molecule in $[Cu^{II}(tren)(H_2O)]Cl_2$ **1**, giving five-co-ordinate $[Cu^{II}(tren)(HAde)]Cl_2$ **2**, whereas the analogous reaction of CuCl, tren and neutral adenine produces $[Cu^{II}(tren)(Ade)]Cl{\cdot}2H_2O$ **4**, whose structure was confirmed by X-ray crystallography.

Infrared Spectra.—Table 2 summarizes the IR absorption spectra of complexes **1**–**4** in comparison with those of free adenine (HAde), tren and the related complexes $[Cu(HAde)_2(ClO_4)_2]{\cdot}EtOH$, $[Ni(Ade)(ClO_4)]{\cdot}EtOH{\cdot}2H_2O$, $[Ni_2(Ade)_3Cl]{\cdot}6H_2O$ and $[Cu(Ade)(HAde)]Cl{\cdot}H_2O$.[10–12] Band assignments refer to data available in the literature for crystalline powders or single crystals (9-methyladenine).[14] High-resolution spectra of adenine isolated molecules have also been obtained at low temperature (11 to 7 K) by using the matrix isolation method,[15] but they are not completely comparable with our data because of the presence of 'the matrix effect'. Nevertheless, those assignments of the strongest bands at 1626 and 1612 cm^{-1} respectively to $\delta(NH_2)$ and to ν(C=C) and ν(C=N) ring mode vibrations,[15] are in accordance with our assignments. With respect to the free ligands, differences are observed in particular in the ν(O–H) and $\nu(NH_2)$ (3400–3100 cm^{-1}), ν(C–H) and ν(N–H) (3000–2550 cm^{-1}) stretching regions and $\delta(NH_2)$(tren) (1700–1600 cm^{-1}) bending regions. Differences are also found in the 1600–1300 and 1300–1200 cm^{-1} regions, in which ν(C=C), ν(C=N), $\gamma(CH_2)$, ring vibrations and ν(C–NH_2), ν(C–N) and ring modes are respectively known to occur. In particular, the ν(N–H) region (2900–2550 cm^{-1}) can indicate whether metal-bonded adenine is present in its neutral or monoanionic form. Neutral adenine-containing complexes show four strong ν(N–H) absorption bands, whereas complexes containing monodeprotonated adenine only exhibit one or two weak maxima in this region.[12] Although the situation is slightly complicated by the presence in the 2990–2800 cm^{-1} range of four $\nu(CH_2)$ stretching frequencies due to the tren ligand, it is reasonable to conclude that in complexes **2** and **3** adenine is co-ordinated to Cu^{II} in its neutral form, whereas in complex **4** it is bound as a monoanionic ligand. Furthermore, the spectra of complexes **2**, **3** and **4** indicate that the adenine N^6H_2 amino group is not involved in metal bonding since the free adenine bands at 1675vs and 1252s cm^{-1}, assigned to symmetrical in-plane and asymmetrical out-of-plane NH_2 deformation modes respectively, only undergo small changes.

As shown in Table 2, the spectra of complexes **2** and **3** are very similar. In fact, apart from specific absorptions due to the NO_3^- anion in the 1370, 825 and 720 cm^{-1} regions, only slight differences are observed in the $\delta(NH_2)$ region (the band of **3** at 1669 cm^{-1} is split into two bands at 1669 and 1661 cm^{-1} in **2**) and in the $\delta(N–H)_{arom}$ region (the shoulder at 1236 cm^{-1} in **3** is resolved as a weak band at 1238 cm^{-1} in **2**), suggesting only a different pattern of hydrogen bonds. Of course, it is not easy to ascertain the metal-binding site of these complexes on the basis of IR spectra alone, but comparison of the frequencies of complexes **2**–**4** shows similar behaviour, in particular for the stretching vibrations of the imidazole and pyrimidine rings,[10] thus suggesting the same metal-binding site for these three complexes. Table 2 also shows that the IR frequencies of the six-co-ordinate complex [Ni(tren)(HAde)Cl]Cl, whose crystal structure revealed adenine co-ordination at the N^3 site,[4] are different from those for the similar Cu^{II} complexes **2** and **3**, indicating that a binding site different from N^3 is involved here even though all these complexes contain adenine as a neutral species.

Moreover, a perfectly trigonal-bipyramidal MX_5 molecule exhibits two IR-active stretching vibrations, ν_3 of symmetry A_2'', and ν_5 of symmetry E′.[16] The distortion from such perfect D_{3h} symmetry, due to constraints in the tren ligand and the presence of the bulky adeninate ligand, causes the appearance of Raman-active stretching absorptions, so that the ν_3 and ν_5 (Cu–N) stretching vibrations split into three IR-active stretching modes and $\nu(Cu–N_{tren})$ absorptions are observed in the 500–430 cm^{-1} region. Lastly, two vibrational frequencies occur at 301m and 260m cm^{-1}, in the region in which Mikulski *et al.*[12] assigned the adenine $\nu(Cu–N_{arom})$ stretching mode in the complex $[Cu(Ade)(HAde)]Cl{\cdot}H_2O$.

Single-crystal Structure of $[Cu^{II}(tren)(Ade)]Cl{\cdot}2H_2O$ **4**.—The crystal contains discrete $[Cu^{II}(tren)(Ade)]^+$ cations, Cl^- anions and water of crystallization molecules which reinforce packing through a complicated hydrogen-bonding network. As shown in Fig. 1, the $[Cu^{II}(tren)(Ade)]^+$ cation has nearly trigonal-bipyramidal geometry, similar to that found for the $[Zn^{II}(tren)Cl]^+$ cation[17] but with some further distortion from trigonal-bipyramidal geometry occurring, for instance, at the N(12)–Cu–N(13) angle, whose large value of 126.8(4)° may be related to accommodating the adeninate ligand. Final atomic coordinates, bond lengths and angles with their estimated standard deviations are reported in Tables 3 and 4.

One interesting feature of this structure is the selective Cu^{II} bonding to the N^9 nitrogen site of monodeprotonated adenine. The Cu–N(9) bond distance of 1.965(9) Å is shorter than that found either in square-pyramidal *fac*-$[Cu^{II}(dien)(Ade)_2]{\cdot}H_2O$ (dien = diethylenetriamine) [mean value 2.017(6) Å][18] or tetrahedral $[Cu^{II}(H_2Ade)_2X_2]X_2$ [2.013(5) Å for X = Br[19] and 2.012(2) Å for X = Cl;[20] H_2Ade^+ = monoprotonated adenine] and is comparable to the $Co^{III}–N^9$ distance of 1.949(3) Å found for *cis*-$[Co^{III}(en)_2(Ade)Cl]Br{\cdot}H_2O$ (en = ethylenediamine).[21] This shortening may be ascribed both to the presence of a negative charge on the adenine molecule and to Cu^{II} five-co-

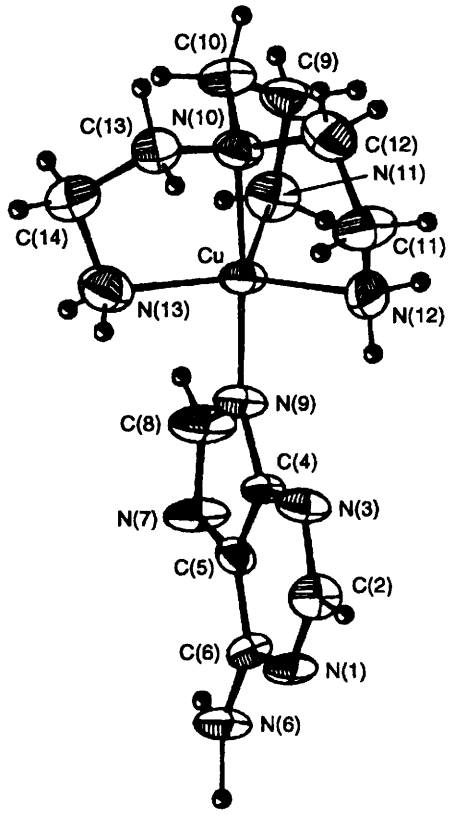

Fig. 1 Molecular structure of the trigonal-bipyramidal $[Cu^{II}(tren)(Ade)]^+$ cation with the atomic numbering scheme used. Thermal ellipsoids are drawn at the 50% probability level

Table 3 Fractional atomic coordinates for $[Cu^{II}(tren)(Ade)]Cl\cdot 2H_2O$ **4** with estimated standard deviations (e.s.d.s) in parentheses

Atom	*X/a*	*Y/b*	*Z/c*
Cu	0.4671(1)	−0.7990(1)	0.2384(1)
N(1)	0.6633(6)	−0.4585(9)	0.0318(6)
N(3)	0.5573(6)	−0.5119(10)	0.1221(6)
N(6)	0.7459(6)	−0.6525(9)	−0.0209(6)
N(7)	0.6415(6)	−0.8866(9)	0.0700(7)
N(9)	0.5420(5)	−0.7936(10)	0.1498(6)
N(10)	0.3960(5)	−0.8016(10)	0.3367(6)
N(11)	0.3939(6)	−1.0125(10)	0.1917(7)
N(12)	0.3828(6)	−0.6030(10)	0.1884(6)
N(13)	0.5807(6)	−0.8042(10)	0.3508(7)
C(2)	0.6026(7)	−0.4193(10)	0.0773(8)
C(4)	0.5769(6)	−0.6666(9)	0.1124(7)
C(5)	0.6372(6)	−0.7227(10)	0.0653(7)
C(6)	0.6832(7)	−0.6128(10)	0.0238(7)
C(8)	0.5833(8)	−0.9167(10)	0.1210(9)
C(9)	0.3225(8)	−1.0292(10)	0.2423(10)
C(10)	0.3601(8)	−0.9650(10)	0.3390(9)
C(11)	0.3465(9)	−0.5432(10)	0.2614(9)
C(12)	0.3182(8)	−0.6846(10)	0.3093(8)
C(13)	0.4611(8)	−0.7585(10)	0.4257(8)
C(14)	0.5533(8)	−0.8353(10)	0.4356(8)
O(1W)	0.5189(6)	0.7221(10)	0.2502(7)
O(2W)	0.8388(7)	−0.0066(9)	0.5665(7)
Cl	1.2991(3)	−0.8481(4)	−0.3896(3)

ordination. In particular, the conformation of *fac*-$[Cu(dien)(Ade)_2]\cdot H_2O$, described as distorted square pyramidal,[18] may be better described as trigonal bipyramidal, like the present complex, since three equatorial sites are occupied by N(10), N(11) and N(9′) and two apical positions by N(9) and N(11).[18] The present complex does not have the usual dimeric or polymeric structure observed for several Cu^{2+} nucleotide base

Table 4 Bond distances (Å) and angles (°) for $[Cu^{II}(tren)(Ade)]Cl\cdot 2H_2O$ **4** with e.s.d.s in parentheses

Cu–N(9)	1.965(9)	Cu–N(10)	2.046(9)
Cu–N(11)	2.124(8)	Cu–N(12)	2.090(8)
Cu–N(13)	2.046(9)	N(1)–C(2)	1.32(2)
N(1)–C(6)	1.35(1)	N(3)–C(2)	1.33(2)
N(3)–C(4)	1.35(1)	N(6)–C(6)	1.34(2)
N(7)–C(5)	1.38(1)	N(7)–C(8)	1.33(2)
N(9)–C(4)	1.38(1)	N(9)–C(8)	1.34(1)
N(10)–C(10)	1.48(1)	N(10)–C(12)	1.50(1)
N(10)–C(13)	1.47(1)	N(11)–C(9)	1.48(2)
N(12)–C(11)	1.44(2)	N(13)–C(14)	1.47(2)
C(4)–C(5)	1.38(2)	C(5)–C(6)	1.40(1)
C(9)–C(10)	1.51(2)	C(11)–C(12)	1.51(2)
C(13)–C(14)	1.50(2)		
N(12)–Cu–N(13)	126.8(4)	N(11)–Cu–N(13)	119.6(4)
N(11)–Cu–N(12)	110.0(4)	N(10)–Cu–N(13)	83.3(4)
N(10)–Cu–N(12)	83.4(4)	N(10)–Cu–N(11)	84.6(4)
N(9)–Cu–N(13)	93.4(4)	N(9)–Cu–N(12)	98.0(4)
N(9)–Cu–N(11)	97.8(4)	N(9)–Cu–N(10)	176.6(4)
C(2)–N(1)–C(6)	119.2(9)	C(2)–N(3)–C(4)	110.7(9)
C(5)–N(7)–C(8)	101.0(8)	Cu–N(9)–C(8)	127.1(6)
Cu–N(9)–C(4)	130.3(7)	C(4)–N(9)–C(8)	102.0(9)
Cu–N(10)–C(13)	107.9(7)	Cu–N(10)–C(12)	108.4(7)
Cu–N(10)–C(10)	107.0(6)	C(12)–N(10)–C(13)	111.2(8)
C(10)–N(10)–C(13)	111.3(8)	C(10)–N(10)–C(12)	110.9(9)
Cu–N(11)–C(9)	107.0(7)	Cu–N(12)–C(11)	108.6(7)
Cu–N(13)–C(14)	110.7(7)	N(1)–C(2)–N(3)	129.4(9)
N(3)–C(4)–N(9)	125.9(9)	N(9)–C(4)–C(5)	108.7(7)
N(3)–C(4)–C(5)	125.4(8)	N(7)–C(5)–C(4)	110.2(8)
C(4)–C(5)–C(6)	118.4(9)	N(7)–C(5)–C(6)	131.4(9)
N(6)–C(6)–C(5)	123.9(9)	N(1)–C(6)–C(5)	116.8(9)
N(1)–C(6)–N(6)	119.3(9)	N(7)–C(8)–N(9)	118.2(9)
N(11)–C(9)–C(10)	109.2(10)	N(10)–C(10)–C(9)	110.6(9)
N(12)–C(11)–C(12)	107.5(9)	N(10)–C(12)–C(11)	110.5(11)
N(10)–C(13)–C(14)	110.4(9)	N(13)–C(14)–C(13)	107.9(9)

complexes, in which bridging adenines link two or three metal ions through N^3 and N^9.[22–24]

Table 5 reports the bond lengths of the five metal–adeninato structures available in the literature containing adenine as a unidentate monoanion bound through N^9. Comparison of the adeninato bond lengths in complex **4** with those of *fac*-$[Cu(dien)(Ade)_2]\cdot H_2O$,[18] *cis*-$[Co(en)_2(Ade)Cl]Br\cdot H_2O$,[21] $[HgMe(Ade)]\cdot H_2O$[27] and *trans*-$[Pd(PBu^n_3)_2(Ade)_2]\cdot 4MeOH$[25] shows good agreement, the highest deviations being lower than 0.03 Å for the three last complexes and slightly higher for *cis*-$[Cu(dien)(Ade)_2]\cdot H_2O$. In particular, the highest deviations are observed for the distances involving N(1) and N(9). These slight differences may be due to a different hydrogen-bonding network. Lastly, the molecular geometry of the Cu(tren) moiety is in accordance with the results obtained from $[Cu(tren)(bzim)][ClO_4]_2$ (bzim = 1-benzylimidazole)[28] and, in particular, it is confirmed here that the Cu–N (tertiary amine) distance is the shortest metal–nitrogen(tren) distance followed by the axial Cu–N(imidazole).

As mentioned above in the IR discussion, complex **4** contains adenine in a rather unusual form, *i.e.* as a unidentate monoanion. This is supported by the following considerations. (*a*) Besides protonation at its original N^9 site, adenine may be protonated at N^1, N^3, N^7. A very sensitive test for recognizing protonated sites is the valence angle at ring nitrogen atoms, which increases by 3–5° upon protonation.[29–32] Table 6 lists the values of these angles for complex **4** in comparison with those found for the adenine monoanion (Ade^-), neutral adenine (HAde, with H at N^9), and mono- (H_2Ade^+, H^+ at N^1) and di-protonated (H_3Ade^{2+}, H^+ at N^1 and N^7) adenine. As may be observed, N^1 or N^7 protonation increases the valence angle by about 5°, whereas the angle values for **4** fit those of the adenine monoanion. Protonation of adenine nitrogen atoms also causes changes in the C–N ring bond lengths, although such variations

are often too small to be diagnostic.[31] (*b*) The most important feature is that the hydrogen-bonding network formed by the adenine monoanion is very different from that formed by HAde, H_2Ade^+ and H_3Ade^{2+}. In fact, Table 7 shows that the N^1, N^3 and N^7 nitrogen atoms are involved in hydrogen bonds as acceptors, thus indicating that they possess an electron lone pair. (*c*) The neutral adenine moiety exhibits a dihedral angle between the imidazole and pyrimidine rings larger than 2°,[33] whereas in complex **4** this angle is 0.81(30)°, indicating almost complete planarity of the adenine skeleton, which parallels its deprotonation. (*d*) The copper ion was ascertained to be a paramagnetic Cu^{II} ion through both EPR and proton NMR spectra, which show clear paramagnetic characteristics. (*e*) No proton attached to N^1, N^3 or N^7 is present in the final Fourier difference synthesis.

The torsion angles for the three $N-CH_2-CH_2-NH_2$ tren helical chains are practically equal, with a mean value of ± 51.2 (1.2)° which is in the normal range, as already discussed.[17]

In conclusion, the synthesis and characterization of these trigonal-bipyramidal $[Cu^{II}(tren)(nucleobase)]X_2$ complexes and in particular the crystal structure determination of $[Cu^{II}(tren)(Ade)]Cl\cdot 2H_2O$ **4** reveal the formation of a selective and exclusive $Cu^{II}-N^9$ bond, whereas the synthesis and X-ray analysis of the octahedral complex $[Ni^{II}(tren)(HAde)Cl]Cl$ demonstrate the formation of a new selective and exclusive $Ni^{II}-N^3$ (adenine) linkage.[4]

Although the adenine N^9 site in DNA is not free for metal-complex binding, being involved in a glycosyl bond, it was interesting to verify the binding affinity among the free adenine nitrogen sites as a function of different metal–tren complexes, with different steric hindrances and co-ordination geometries, and in particular, to examine whether the selective N^3 pyrimidine site[4] found in the bulky six-co-ordinate complex [Ni(tren)(HAde)Cl]Cl, occurs preferentially or not in the analogous five-co-ordinate Cu^{II} complex with lower steric hindrance. The present results support the important role of steric hindrance and co-ordination geometry in recognizing a pre-determined nitrogen donor site in DNA nucleobases. Moreover, it appears that once the N^9 site of the free adenine present in animal cells is involved in Cu^{II}–tren bonding, the formation of AMP by adenine phosphoribosyltransferase is probably inhibited. Further studies on adenine metal-complex binding will be carried out using N^9 substituted adenine or adenine nucleotides directly.

Experimental

Infrared spectra were measured as KBr pellets or Nujol mulls on a Nicolet 5Sxc FT-IR (20 far IR) spectrometer. The UV/VIS spectra were measured in ethanol solutions on Perkin-Elmer Lambda 15 and Beckman DK-2A spectrophotometers. Thermogravimetric measurements were carried out on a Perkin-Elmer TGS-2 analyser equipped with a Fourier-transform IR (Bruker IFS-66) spectrometer. The EPR measurements were performed on crystalline samples using a Bruker ER 200D X-band spectrometer (equipped with nitrogen gas cryostat). Proton NMR spectra were recorded on a model FX 90Q, JEOL FT spectrometer at 296 K in CD_3OD, using $SiMe_4$ as internal standard.

Synthesis of $[Cu^{II}(tren)(H_2O)]Cl_2$ **1**.—To an emerald green ethanol solution (40 cm^3) of $CuCl_2\cdot 2H_2O$ (1.278 g, 7.5 mmol), tren (1.15 cm^3, 7.5 mmol) was added, dissolved in the same solvent (10 cm^3). The colour changed to blue and the solution was stirred at room temperature for 2 h. The addition of diethyl ether precipitated a blue compound, which was filtered off, washed with a EtOH–Et_2O (1:2 v/v) and dried under vacuum.

Table 5 Comparison of bond lengths (Å) in N^9 unidentate monoanion of adenine

	a	*b* (mean value)	*c*	*d*	*e*
N(1)–C(2)	1.32(2)	1.333(11)	1.344(5)	1.33(2)	1.332(6)
N(1)–C(6)	1.35(1)	1.293(11)	1.377(5)	1.36(2)	1.351(6)
N(3)–C(2)	1.33(2)	1.322(11)	1.333(5)	1.33(2)	1.326(5)
N(3)–C(4)	1.35(1)	1.300(11)	1.369(5)	1.35(2)	1.366(5)
C(4)–C(5)	1.38(2)	1.387(10)	1.384(5)	1.37(2)	1.378(5)
C(5)–C(6)	1.40(1)	1.373(11)	1.414(5)	1.40(2)	1.412(5)
N(6)–C(6)	1.34(2)	1.366(10)	1.352(5)	1.34(2)	1.346(5)
N(7)–C(5)	1.38(1)	1.331(11)	1.383(5)	1.38(2)	1.373(5)
N(7)–C(8)	1.33(2)	1.350(10)	1.340(5)	1.35(2)	1.319(5)
N(9)–C(4)	1.38(1)	1.334(10)	1.371(5)	1.36(2)	1.356(5)
N(9)–C(8)	1.34(1)	1.330(11)	1.341(5)	1.38(2)	1.359(5)

[a] $[Cu(tren)(Ade)]Cl\cdot 2H_2O$ **4**. [b] *fac*-$[Cu(dien)(Ade)_2]\cdot H_2O$, ref. 18. [c] *cis*-$[Co(en)_2(Ade)Cl]Br\cdot H_2O$, ref. 21. [d] $[HgMe(Ade)]\cdot H_2O$, ref. 27. [e] *trans*-$[Pd(PBu^n_3)_2(Ade)_2]\cdot 4MeOH$, ref. 25. Although some other complexes containing the monoanion are known, they are not reported here, due to adenine positional disorder or the presence of bridging chelated adenine, refs. 22 and 26.

Table 7 Possible intermolecular hydrogen bonds (Å) and angles (°)

D–H···A[a]	D–H	D···A	H···A	Angle (°)
O(W1)–H(1W1)···N(3^{I})	1.16(1)	2.92(1)	1.85(1)	152.3(6)
O(W1)–H(2W1)···Cl^{II}	0.79(1)	3.14(1)	2.37(1)	163.4(7)
O(W2)–H(1W2)···Cl^{III}	1.08(1)	3.14(1)	2.19(1)	145.6(4)
N(13)–H(2)N(13)···O($W2^{IV}$)	0.91(1)	2.91(1)	2.07(1)	152.1(7)
O(W2)–H(2W2)···Cl^{V}	1.10(1)	3.15(1)	2.77(1)	100.1(5)
N(6)–H(1)N(6)···N(7^{VI})	1.09(1)	3.02(1)	1.94(1)	167.6(5)
N(6)–H(2)N(6)···N(1^{VII})	1.15(1)	2.94(1)	1.98(1)	139.5(6)
N(11)–H(2)N(11)···O($W1^{VIII}$)	0.89(1)	2.90(1)	2.02(1)	169.6(7)
N(12)–H(2)N(12)···N(1^{IX})	0.92(1)	3.23(1)	2.70(1)	118.0(6)
N(13)–H(1)N(13)···Cl^{X}	0.88(1)	3.40(1)	2.63(1)	147.5(6)

[a] Equivalent positions: I, $x, y + 1, z$; II, $-x + 2, -y, -z$; III, $-x + 2, -y - 1, -z$; IV, $-x + \frac{1}{2} + 1, y - \frac{1}{2}, -z + 1$; V, $x - \frac{1}{2}, -y - \frac{1}{2}, z + 1$; VI, $-x + \frac{1}{2} + 1, y + \frac{1}{2}, -z$; VII, $-x + \frac{1}{2} + 1, y - \frac{1}{2}, -z$; VIII, $x, y - 2, z$; IX, $-x + 1, -y - 1, -z$; X, $-x + 2, -y - 2, -z$.

Table 6 Valence angles (°) at the ring nitrogen atoms in the adenine monoanion (Ade^-), neutral adenine (HAde), monoprotonated (H_2Ade^+) and diprotonated adenine (H_3Ade^{2+})

	Ade^-						
	a	*b*	*c* (mean value)	d	HAde[e] H at N^9	H_2Ade^+[f] H at N^9, N^1	H_3Ade^{2+}[g] H at N^9, N^1, N^7
C(2)–N(1)–C(6)	119.2(9)	119.0(7)	118.1	118.8(3)	119.8	123.6	124.0
C(2)–N(3)–C(4)	110.7(9)	110.8(7)	111.6	111.2(4)	111.0	112.1	111.8
C(5)–N(7)–C(8)	101.0(8)	102.6(7)	101.8	103.0(3)	104.4	103.5	107.3
C(4)–N(9)–C(8)	102.0(9)	102.4(6)	103.6	104.3(3)	104.8	105.6	107.9

[a] $[Cu(tren)(Ade)]Cl\cdot 2H_2O$ **4**. [b] *fac*-$[Cu(dien)(Ade)_2]\cdot H_2O$, ref. 18. [c] *cis*-$[Co(en)_2(Ade)Cl]Br\cdot H_2O$, ref. 21. [d] *trans*-$[Pd(PBu^n_3)_2(Ade)_2]\cdot 4MeOH$, ref. 25. [e] Average of a number of adenine structures, ref. 33. [f] Average of five structures, ref. 34. [g] Average of three structures, ref. 31.

Table 8 Crystallographic data for $[Cu^{II}(tren)(Ade)]Cl\cdot 2H_2O$ **4**

Formula	$C_{11}H_{26}ClCuN_9O_2$
M	415.39
Crystal size/mm	0.20 × 0.20 × 0.10
Colour, habit	Blue-green, prism
Crystal system	Monoclinic
Space group	$P2_1/a$
a/Å	15.001(2)
b/Å	8.422(1)
c/Å	15.039(2)
β/°	105.90(6)
U/Å^3	1827.3(7)
Z	4
D_c/g cm^{-3}	1.510
μ(Mo-Kα)/cm^{-1}	13.684
F(000)	868
θ_{max}/°	25.0
Measured reflections	5110
Unique reflections	2596
Indices explored (max.)	$\pm h$ (±28), $\pm k$ (±10), $+l$ (+21)
Indices of observed and merged reflections	$\pm h$ (±16), $+k$ (+10), $+l$ (+17)
Merging R (based on I)	0.015
Data with $F_o > 4\sigma(F_o)$	1524
Parameters refined	217
R	0.065
R'	0.063
Goodness-of-fit	1.261
Weighting scheme	$w = 1/[\sigma^2(F) + 0.001\,622F^2]$
Largest shift/e.s.d.	0.12
Highest peak in difference map/e Å^{-3}	0.8

Yield 2.04 g, 91% (Found: C, 24.10; H, 6.70; Cl, 23.65; N, 18.60. Calc. for $C_6H_{20}Cl_2CuN_4O$: C, 24.10; H, 6.75; Cl, 23.75; N, 18.75%).

The assignment of the molecular structure was supported by UV/VIS and IR spectra and, in particular, by thermogravimetric measurements. The loss of H_2O from the complex (dehydration) took place between 428 and 499 K with a mass loss of 6.75% (6.03% theoretical). The resulting gas was also identified as water vapour by its vibrational and rotational spectra. From 499 to 746 K decomposition occurred, with loss of tren and chlorine (mass loss 58.82%, theoretical 60.90%) leading to the formation of CuO.

Synthesis of $[Cu^{II}(tren)(HAde)]Cl_2$ **2**.—To an ethanol solution of $[Cu^{II}(tren)(H_2O)]Cl_2$ (0.597 g, 2.0 mmol in 40 cm^3), adenine (0.270 g, 2.0 mmol) was added, previously refluxed to dissolution in 70 cm^3 of the same solvent. The solution was stirred at room temperature for 1 h and the solvent then allowed to evaporate slowly. The blue-green precipitate was filtered off, washed with EtOH–Et_2O (1:2 v/v) and dried under vacuum. Yield 0.71 g, 85% (Found: C, 32.10: H, 5.75; Cl, 16.95; N, 30.55. Calc. for $C_{11}H_{23}Cl_2CuN_9$: C, 31.75; H, 5.55; Cl, 17.05; N, 30.30%).

Synthesis of $[Cu^{II}(tren)(HAde)][NO_3]_2$ **3**.—To a stirred pale blue solution of $Cu(NO_3)_2\cdot 2.5H_2O$ (0.281 g, 1.21 mmol) in a mixture of water (13 cm^3) and ethanol (10 cm^3) an aqueous solution (10 cm^3) of tren (0.18 cm^3, 1.21 mmol) was added. The reaction mixture suddenly turned blue. After about 30 min adenine (0.163 g, 1.21 mmol) dissolved in hot water (180 cm^3) was added slowly under stirring. Aliquots of NaOH were added until the pH of the solution was 7.0. The mixture was refluxed at 60 °C for 8 h. The solution was allowed to concentrate slowly at room temperature. A pale blue powder precipitated, which was separated by filtration, washed with H_2O and EtOH, and dried under vacuum. Yield 0.48 g, 84% (Found: C, 28.60; H, 5.00; N, 32.30. Calc. for $C_{11}H_{23}CuN_{11}O_6$: C, 28.15; H, 4.95; N, 32.85%).

Synthesis of $[Cu^{II}(tren)(Ade)]Cl\cdot 2H_2O$ **4**.—This complex was prepared by adding tren (0.35 cm^3, 2.29 mmol) in ethanol (20 cm^3) to CuCl (0.226 g, 2.29 mmol) dissolved under stirring in 100 cm^3 of the same solvent. After about 30 min adenine (0.309 g, 2.29 mmol) dissolved in ethanol (100 cm^3) by refluxing for 1 h, was added slowly under stirring and the solution then allowed to cool. Slow evaporation of the ethanol from the blue-green solution at room temperature after 4 weeks gave blue-green crystals, which were isolated, washed and air-dried. Yield 0.74 g, 78% (Found: C, 31.85; H, 6.30; Cl, 8.50; N, 30.45. Calc. for $C_{11}H_{26}ClCuN_9O_2$: C, 31.80; H, 6.30; Cl, 8.55; N, 30.35%).

Single-crystal Structural Determination of $[Cu^{II}(tren)(Ade)]Cl\cdot 2H_2O$ **4**.—Crystallographic data and collection and structure refinement details are given in Table 8. A suitable crystal was mounted on a glass capillary (slightly coated with diluted polystyrene cement) on a Philips PW1100 diffractometer equipped with graphite-monochromated Mo-Kα radiation. 5110 Reflections were collected in the ω–2θ mode to $2\theta_{max}$ = 50°, exploring several quadrants of reciprocal space, and were then merged to give 2596 independent reflections. The internal consistency index (based on I) was 0.015, indicating good agreement between equivalent reflections. Intensity data were collected at 293 K and Lorentz and polarization corrections were applied. Absorption corrections were deemed unnecessary due to the low values of the internal consistency index and linear absorption coefficient (μ) and the small size of the crystal. The structure was solved by the standard Patterson method and successive Fourier maps, and was refined by the full-matrix least-squares method using anisotropic thermal parameters for non-H atoms and isotropic ones for H atoms. All crystallographic calculations were performed with the SHELX 76[35] and PARST[36] set of programs and the molecular illustration was drawn using ORTEPII.[37]

Additional material available from the Cambridge Crystallographic Data Centre comprises H-atom coordinates, thermal parameters and remaining bond lengths and angles.

Acknowledgements

This research was performed with the support of the Ministero dell'Università e della Ricerca Scientifica (MURST), Rome (Italy).

References

1 R. B. Martin and Y. H. Mariam, *Met. Ions Biol. Syst.*, 1979, **8**, 57.
2 E. Sletten and B. Thorstensen, *Acta Crystallogr., Sect. B*, 1974, **30**, 2438; R. Beyerle-Pfnur, B. Brown, R. Faggiani, B. Lippert and C. J. L. Lock, *Inorg. Chem.*, 1985, **24**, 4001.
3 L. M. Torres and L. G. Marzilli, *J. Am. Chem. Soc.*, 1991, **113**, 4678.
4 A. Marzotto, D. A. Clemente, A. Ciccarese and G. Valle, *J. Crystallogr. Spectrosc. Res.*, 1993, **23**, 119.
5 A. Marzotto, D. A. Clemente and G. Valle, *Acta Crystallogr., Sect. C*, 1993, **49**, 1252.
6 N. Kamatani and D. A. Carson, *Biochim. Biophys. Acta*, 1981, **675**, 344; J. M. Wilson, T. E. O'Toole, P. Argos, D. S. Shewach, P. E. Daddona and W. N. Kelley, *J. Biol. Chem.*, 1986, **261**, 13677.
7 D. D. Roberts and I. J. Goldstein, *J. Biol. Chem.*, 1983, **258**, 13820.
8 M. Ciampolini and N. Nardi, *Inorg. Chem.*, 1966, **5**, 41.
9 M. Duggan, N. Ray, B. Hathaway, G. Tomlinson, P. Brint and K. Pelin, *J. Chem. Soc., Dalton Trans.*, 1980, 1342 and refs. therein.
10 A. N. Speca, C. M. Mikulski, F. J. Iaconianni, L. L. Pytlewski, N. M. Karayannis, *J. Inorg. Nucl. Chem.*, 1981, **11**, 2771.
11 R. Savoie, J.-J. Jutier, L. Prizant and A. L. Beauchamp, *Spectrochim. Acta, Part A*, 1982, **38**, 561.
12 C. M. Mikulski, S. Cocco, N. De Franco and T. Moore, *Inorg. Chim. Acta*, 1985, **106**, 98.
13 M. A. Ficheux and J. H. Morris, *Bull. Soc. Chim. Fr.*, 1978, 581.
14 Y. Kyogoku, S. Higuchi and M. Tsuboi, *Spectrochim. Acta, Part A*, 1967, **23**, 969.

15 S. G. Stepanian, G. G. Sheina, E. D. Radchenko and Yu. P. Blagoi, *J. Mol. Struct.*, 1985, **131**, 333; M. J. Nowak, L. Lapinski, J. S. Kwiatkowski and J. Leszczynski, *Spectrochim. Acta, Part A*, 1991, **47**, 87.
16 K. Nakamoto, *Infrared Spectra of Inorganic and Coordination Compounds*, Wiley, New York, 1963.
17 A. Marzotto, D. A. Clemente and G. Valle, *Acta Crystallogr., Sect. C*, 1994, **50**, 1451.
18 H. Sakaguchi, H. Anzai, K. Furuhata, H. Ogura, Y. Iitaka, T. Fujita and T. Sakaguchi, *Chem. Pharm. Bull.*, 1978, **26**, 2465.
19 P. de Meester and A. C. Skapski, *J. Chem. Soc., Dalton Trans.*, 1973, 424.
20 D. B. Brown, J. W. Hall, H. M. Helis, E. G. Walton, D. J. Hodgson and W. E. Hatfield, *Inorg. Chem.*, 1977, **16**, 2675.
21 T. J. Kistenmacher, *Acta Crystallogr., Sect. B*, 1974, **30**, 1610.
22 E. Sletten, *Acta Crystallogr., Sect. B*, 1969, **25**, 1480; 1970, **26**, 1609.
23 P. de Meester and A. C. Skapski, *Inorg. Phys. Theor.*, 1971, 1480.
24 P. de Meester and A. C. Skapski, *J. Chem. Soc., Dalton Trans.*, 1972, 2400.
25 W. M. Beck, J. C. Calabrese and N. D. Kottmair, *Inorg. Chem.*, 1979, **18**, 176.
26 T. J. Kistenmacher, *Acta Crystallogr., Sect. B*, 1973, **29**, 1974.
27 L. Prizant, M. J. Olivier, R. Rivest and A. L. Beauchamp, *Can. J. Chem.*, 1981, **59**, 1311.
28 R. T. Stibrany, J. A. Potenza and H. J. Schugar, *Acta Crystallogr., Sect. C*, 1993, **49**, 1561.
29 C. Singh, *Acta Crystallogr.*, 1965, **19**, 861.
30 E. D. Ringerty, *The Purines—Theory and Experiment*, eds. E. D. Bergmann and B. Pullmann, Israel Academy of Sciences, Jerusalem, 1972.
31 G. L. Hardgrove Jun., J. R. Einstein, B. E. Hingerty and C. H. Wei, *Acta Crystallogr., Sect. C*, 1983, **39**, 88.
32 R. Taylor and O. Kennard, *J. Mol. Struct.*, 1982, **78**, 1.
33 D. Voet and A. Rich, *Prog. Nucleic Acid Res. Mol. Biol.*, 1970, **10**, 183.
34 B. E. Hingerty, J. R. Einstein and C. H. Wei, *Acta Crystallogr., Sect. B*, 1981, **37**, 140.
35 G. M. Sheldrick, SHELX 76, Program for crystal structure determination, University of Cambridge, 1976.
36 M. Nardelli, *Comput. Chem.*, 1983, **7**, 95.
37 C. K. Johnson, ORTEPII, Report ORNL-5138, Oak Ridge National Laboratory, TN, 1976.

Received 28*th September* 1994; *Paper* 4/05919K